A core-top calibration of B/Ca in the benthic foraminifers *Nuttallides umbonifera* and *Oridorsalis umbonatus*: A proxy for Cenozoic bottom water carbonate saturation

Rachel E. Brown [a,*], Linda D. Anderson [b], Ellen Thomas [c,d], James C. Zachos [a]

[a] Earth and Planetary Sciences Department, University of California, Santa Cruz, CA 95064, United States
[b] Institute of Marine Sciences, University of California, Santa Cruz, CA 95064, United States
[c] Yale University, Department of Geology & Geophysics, New Haven, CT 06520, United States
[d] Wesleyan University, Department of Earth & Environmental Sciences, Middletown, CT 06459, United States

ABSTRACT

We present modern B/Ca core-top calibrations for the epifaunal benthic foraminifer *Nuttallides umbonifera* and the infaunal *Oridorsalis umbonatus* to test whether B/Ca values in these species can be used for the reconstruction of paleo-$\Delta[CO_3^{2-}]$. *O. umbonatus* originated in the Late Cretaceous and remains extant, whereas *N. umbonifera* originated in the Eocene and is the closest extant relative to *Nuttallides truempyi*, which ranges from the Late Cretaceous through the Eocene. We measured B/Ca in both species in 35 Holocene sediment samples from the Atlantic, Pacific and Southern Oceans. B/Ca values in epifaunal *N. umbonifera* (~85–175 µmol/mol) are consistently lower than values reported for epifaunal *Cibicidoides (Cibicides) wuellerstorfi* (130–250 µmol/mol), though the sensitivity of $\Delta[CO_3^{2-}]$ on B/Ca in *N. umbonifera* (1.23 ± 0.15) is similar to that in *C. wuellerstorfi* (1.14 ± 0.048). In addition, we show that B/Ca values of paired *N. umbonifera* and its extinct ancestor, *N. truempyi,* from Eocene cores are indistinguishable within error. In contrast, both the B/Ca (35–85 µmol/mol) and sensitivity to $\Delta[CO_3^{2-}]$ (0.29 ± 0.20) of core-top *O. umbonatus* are considerably lower (as in other infaunal species), and this offset extends into the Paleocene. Thus the B/Ca of *N. umbonifera* and its ancestor can be used to reconstruct bottom water $\Delta[CO_3^{2-}]$, whereas *O. umbonatus* B/Ca appears to be buffered by porewater $[CO_3^{2-}]$ and suited for constraining long-term drift in seawater B/Ca.

© 2011 Elsevier B.V. All rights reserved.

1. Introduction

The major climatic shifts of earth's recent and deep past, ranging from the glacial–interglacial cycles of the Pleistocene to the thermal maxima of the early Cenozoic, have largely been attributed to systematic changes in the concentration of CO_2 in the atmosphere (e.g., Dickens et al., 1997; Shackleton, 2000). Changes in atmospheric pCO_2, ranging from tens to hundreds of ppmv, should have been manifested in measurable shifts in the carbonate chemistry of seawater, specifically pH and $[CO_3^{2-}]$ (Zeebe and Wolf-Gladrow, 2001). An ability to quantify the $[CO_3^{2-}]$ of paleo seawater, particularly within the deep sea, is thus key to reconstructing changes in the content and distribution of carbon in the oceans and atmosphere, and to evaluating the contribution of changes in concentration of atmospheric carbon to past climate change (e.g., Yu et al., 2010a; Zeebe et al., 2009). Moreover, knowledge of the carbonate saturation of past oceans is essential to identifying the range within which

calcifying marine organisms could potentially tolerate future ocean acidification (Fabry et al., 2008; Feely, 2004; Riebesell et al., 2000).

Attempts to constrain past deep-sea $[CO_3^{2-}]$ include, for example, measurements of foraminiferal test weight (Broecker and Clark, 2003; Lohmann, 1995), the $CaCO_3$ size index (Broecker and Clark, 1999), calcite crystallinity (Bassinot et al., 2004), foraminiferal Zn/Ca (Marchitto et al., 2000, 2002), and foraminiferal B/Ca (Yu et al., 2008; Yu and Elderfield, 2007). In aqueous solutions, the equilibrium distribution of boric acid ($[B(OH)_3]$) and the borate ion ($[B(OH)_4^-]$) is strongly pH dependent. At low pH (<7) virtually all boron is present in the form of boric acid, whereas at high pH (>10) boron exists predominantly in the form of borate. B/Ca in calcite thus could potentially serve as a pH proxy because the borate ion and not boric acid is incorporated into the foraminiferal calcite lattice (Hemming and Hanson, 1992). This appears to work for planktonic foraminifers (Yu et al., 2007a), but in benthic foraminifera, B/Ca depends upon $\Delta[CO_3^{2-}]$ (where $\Delta[CO_3^{2-}] = [CO_3^{2-}] - [CO_3^{2-}]_{sat}$) (Yu and Elderfield, 2007). Despite large intra-species variations, B/Ca in individual species of benthic foraminifera lies within a relatively small range linearly correlated with deep water $\Delta[CO_3^{2-}]$ (Yu and Elderfield, 2007). The correlation between B/Ca and $\Delta[CO_3^{2-}]$ exists even at high $\Delta[CO_3^{2-}]$, in contrast with other deep-sea carbonate ion proxies (e.g. calcite

* Corresponding author.
  E-mail address: rbrown@ucsc.edu (R.E. Brown).

crystallinity and Zn/Ca; Bassinot et al., 2004; Marchitto et al., 2000, 2002).

The two modern benthic foraminiferal species with robust B/Ca calibrations, *Cibicidoides (Cibicides,* Schweizer, 2006*) wuellerstorfi* and *C. mundulus* (Yu et al., 2010b; Yu and Elderfield, 2007), cannot be used to assess $\Delta[CO_3^{2-}]$ during the extreme greenhouse events of the early Cenozoic, as neither extends back beyond the Oligocene (van Morkhoven et al., 1986). We have therefore completed a B/Ca core-top calibration for the longer-lived cosmopolitan species *Nuttallides umbonifera,* the closest extant relative to *Nuttallides truempyi* and a common Upper Cretaceous–Paleogene species (Kaiho, 1998), and *Oridorsalis umbonatus,* which evolved in the Late Cretaceous and is extant (Kaiho, 1998). *N. umbonifera* is common in bottom waters at the low end of the saturation spectrum (i.e., Pacific, Bremer and Lohmann, 1982). Our results show that B/Ca in *N. umbonifera,* but not in *O. umbonatus,* is significantly correlated with deep-water saturation state and can be used for paleo-reconstructions. We also assess the sensitivity of benthic B/Ca partitioning to other environmental parameters such as bottom water temperature (BWT), pH, and the borate to bicarbonate ratio using principal component analysis and principal components regression. Finally, we show that during the middle Eocene, when *N. umbonifera* coexisted with its ancestor *N. truempyi,* the two species recorded similar B/Ca ratios, with an offset to *O. umbonatus* that is within the range observed in core-tops.

2. Samples, methods and data sources

2.1. Samples

The B/Ca of the epifaunal benthic foraminifer *N. umbonifera* and the shallow infaunal *O. umbonatus* were measured in 35 Holocene core-top sediment samples from the Atlantic, Pacific and Southern Oceans (Fig. 1). Most samples are from box and multicores collected from abyssal water depths (~3200 to 4900 m, Supplementary Table S1–S3). To verify that core-top sediments were not contaminated by pre-Holocene specimens, we also measured the $\delta^{18}O$ and $\delta^{13}C$ values of the benthic foraminifer *C. wuellerstorfi,* which commonly co-occurs with *N. umbonifera* and *O. umbonatus.* Samples with *C. wuellerstorfi* $\delta^{18}O > 4‰$ (n = 6) were rejected as possibly reflecting partial contamination by reworked glacial specimens. We also excluded two samples from core depths likely to be greater than Holocene in age.

For the paleo part of this investigation, we analyzed co-occurring specimens of *N. truempyi*, *N. umbonifera*, and *O. umbonatus* from a set of 7 middle Eocene samples from ODP Sites 689 and 690, Maud Rise (Supplementary Table S4). We also analyzed co-existing specimens of *N. truempyi* and *O. umbonatus* from the upper Paleocene-lower Eocene sections of ODP Sites 1209 on Shatsky Rise, Pacific, and 1263 on Walvis Ridge, south Atlantic.

2.2. Analytical methods

2.2.1. B/Ca

For each sample, ~10–20 tests (~100–200 μg) of each species were picked, largely from the 150–250 μm size fraction, then crushed and cleaned following the methods of Boyle and Keigwin (1985/1986) as revised by Martin and Lea (2002). Cleaning included multiple ultrasonication steps in boron-clean Milli-Q water (obtained from a Milli-Q Academic water purification system with Q-gard boron purification pack and Quantum ICP) and methanol, as well as an oxidative and reductive step. The reductive cleaning step does not affect B/Ca by preferential dissolution (Yu et al., 2007) and was included so we could monitor other trace element ratios (e.g., Mg/Ca). All sample handling following crushing was done in a laminar flow bench using acid-cleaned plastic-ware.

We measured B/Ca along with other elemental ratios by inductively coupled plasma mass spectrometer (ICP-MS; Finnegan Element XR) using a combination of techniques detailed in Rosenthal et al. (1999), Yu et al. (2005) and Al-Ammar et al. (1999, 2000). The masses analyzed were ^{11}B and ^{43}Ca. The cleaned tests were dissolved in 350–400 mL 0.075 N HNO$_3$ (depending on initial sample weight) and free-aspirated with a Teflon nebulizer (APEX PFA ST-1255) into a Teflon spray chamber (ES-2100-5471 47 mm PFA). We measured B blanks on the same acid as used for sample dissolution, and monitored intra-run variability with liquid consistency standards (B/Ca = 74 μmol/mol) as well as with a solid foraminiferal consistency standard composed of crushed and homogenized *Globigerinoides sacculifer* from core-top KNR 110 2–58 STN40-2 (without final sac; B/Ca = 92 ± 8 μmol/mol). Based on replicate measures of the consistency standard, within-run precision is <1% (RSD) and between-run precision is <5% (RSD) for B/Ca.

Measurements of B/Ca in foraminiferal calcite by ICP-MS may be compromised by high boron blanks, a memory effect, and a calcium

Fig. 1. Locations of core-tops used in this study, the majority of which are box and multi cores. Water depths range between ~3300 and 4900 m. Map generated using planiglobe (http://www.planiglobe.com).

matrix effect (e.g. Al-Ammar et al., 1999, 2000; Yu et al., 2005). High boron background levels as well as the memory effect arise largely because boron tends to volatilize from the sample solution as boric acid, collecting in droplets inside the spray chamber (Wara et al., 2003; Yu et al., 2005). The memory effect can be partly minimized by allocating longer washout and uptake times; washout times were set to 30 s and uptake time to 40 s. In addition, ammonia gas injected into the spray chamber at 5 mL/min (Al-Ammar et al., 1999, 2000; Wara et al., 2003) raises the pH of the droplets enough to change the speciation of the boron to borate, which is not volatile. This modification effectively reduced the B blank from >20% of our consistency standard to a stable 0.4 ppb (<10%). Although this is a relatively high blank, the blank remained stable throughout the run ($\pm 4\%$), and thus our liquid consistency standard precision was <2%. To minimize the matrix effect, Yu et al. (2005) diluted all samples to the same calcium concentration, which requires the removal of an aliquot for separate analysis. Small sample sizes prevented our use of this procedure. Instead we monitored the matrix effect by monitoring Ca concentrations ([Ca]) using the same suite of standards from which we constructed calibration curves (following the method employed by de Villiers et al., 2002; Yu et al., 2005). The [Ca]-calibration curves determined from multiple standards are linear and R^2-values are usually greater than 0.999. Values were rejected when [Ca] fell outside the range of concentrations in our standards. Drift correction standards and blanks were analyzed every 5 samples.

2.2.2. Stable isotopes

We measured carbon and oxygen isotopic ratios on 2–5 C. wuellerstorfi tests from the 150–250 μm size fraction of each core-top on a PRISM mass spectrometer at the UCSC Stable Isotope Laboratory facilities. Data are reported using delta (δ) notation and referenced to Vienna Peedee belemnite. Analytical precision based on replicate measurements of in-house standard Carrara Marble and NBS-19 is 0.02‰ (1σ) for $\delta^{13}C$ and 0.03‰ (1σ) for $\delta^{18}O$.

2.3. Hydrographic data

We estimated site-specific hydrographic data (Supplementary Table S1–S3), including bottom water temperature (BWT), salinity, total dissolved inorganic carbon (DIC), total alkalinity (ALK), and nutrient levels (PO_4 and SiO_3), from data in the Global Ocean Data Analysis Project (GLODAP) (Key et al., 2004) and the Carbon in Atlantic Ocean (CARINA) project (e.g. Key et al., 2010). After correcting for the anthropogenic CO_2 contribution to DIC (when required), we computed the pre-industrial carbonate chemistry using the CO_2sys.xls program of Pelletier et al. (2007) in accordance with standard protocol (e.g. Foster, 2008; Yu and Elderfield, 2007). We quantified the uncertainty in our estimates of $\Delta[CO_3^{2-}]$, pH and BWT for each core-top site by locating all GLODAP and/or CARINA sites within two degrees of latitude and longitude of each core-top site where possible, and up to five degrees where data are scarce (<3 stations), averaged the $\Delta[CO_3^{2-}]$, pH and BWTs in that group to generate a value for each core-top site, and finally bootstrapped each variable to generate estimates of standard error (Efron, 1979).

2.4. Statistical analyses

For our small Holocene-to-modern data set ($n=27$), we found that the slope of the regression line between B/Ca and all parameters investigated is highly sensitive to the incorporation of error in both axes, i.e. the analytical error associated with the measurement of B/Ca as well as the error associated with estimating seawater $\Delta[CO_3^{2-}]$ at the core-top sites. We used a bivariate least squares regression (Cantrell, 2008; Reed, 1989; York, 1969; York et al., 2004) programmed in Microsoft Excel by Kromer (http://vizsage.com/other/leastsquaresexcel/) to incorporate these errors in both axes.

We also evaluated the sensitivity of B/Ca to a number of hydrographic parameters (e.g. pH, BWT, $[B(OH)_4^-]/[HCO_3^-]$ as well as $\Delta[CO_3^{2-}]$) by performing principal component analysis and principal component regression (Supplementary material, Supplementary Table S5).

3. Results

3.1. Core-top $\delta^{13}C$ and $\delta^{18}O$

Core-top benthic C. wuellerstorfi $\delta^{13}C$ values range between ~−0.2–1‰ and are positively correlated with $\Delta[CO_3^{2-}]$ ($R^2 = 0.56$, $p < .001$) as well as with N. umbonifera B/Ca ($R^2 = 0.42$, $p = .0012$) (Fig. 2). Core-top $\delta^{18}O$ values generally range between ~2.8–3.8‰.

3.2. Core-top B/Ca

N. umbonifera and O. umbonatus B/Ca values display large intra-species differences, similar to those observed by Yu and Elderfield (2007). B/Ca values range from ~35–60 μmol/mol in O. umbonatus and ~85–175 μmol/mol in N. umbonifera (Figs. 3, 4, 5). N. umbonifera B/Ca values are offset from those in C. wuellerstorfi (130–225 μmol/mol; Yu and Elderfield, 2007) by a near constant number (~50 μmol/mol),
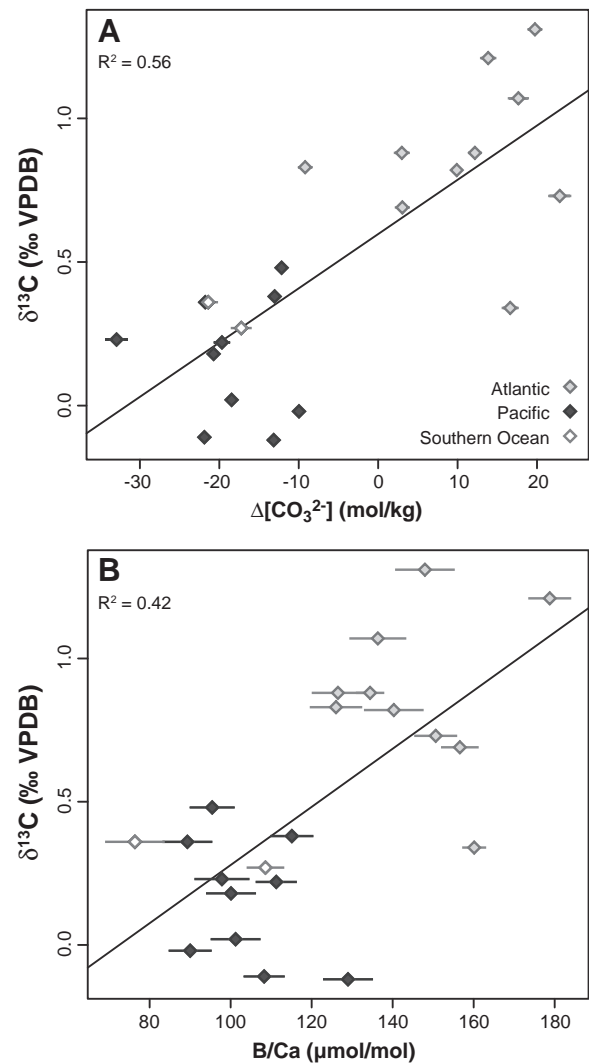
Fig. 2. Correlation between core-top $\delta^{13}C$ (C. wuellerstorfi) and (A) seawater $\Delta[CO_3^{2-}]$ (B) benthic foraminiferal B/Ca ratio (N. umbonifera). $\delta^{13}C$ significantly predicts B/Ca ratios (slope = 0.0102, $R^2 = 0.42$, $p = .0012$) as well as seawater $\Delta[CO_3^{2-}]$ (slope = 0.019, $R^2 = 0.56$, $p < .001$). Vertical error bars ($1\sigma = \pm 0.02$‰) are smaller than the size of the points.
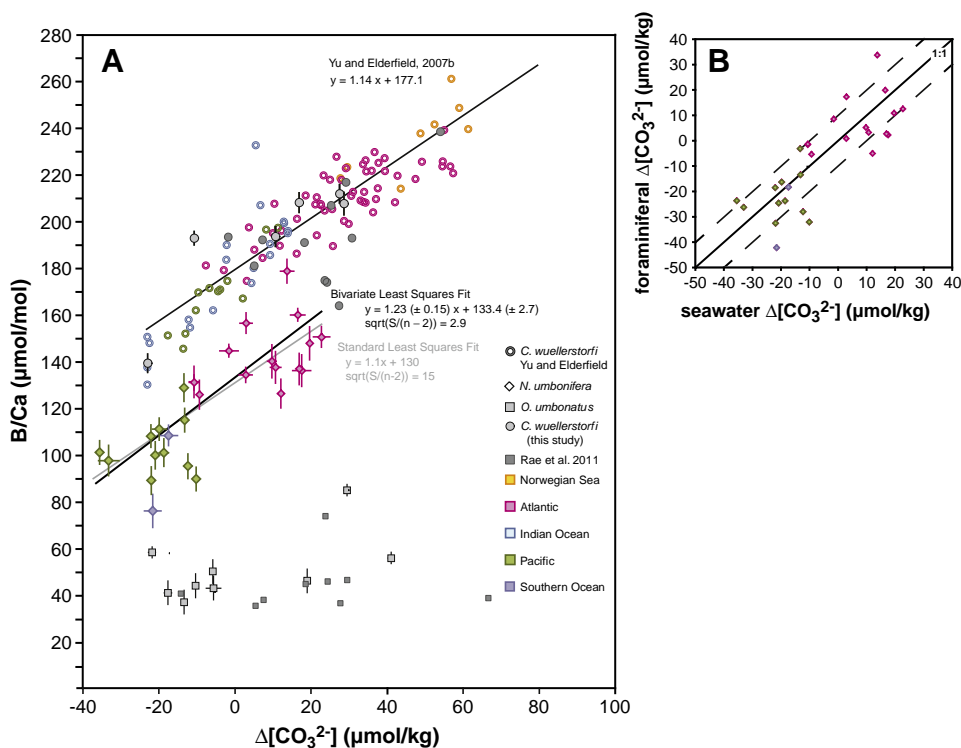
Fig. 3. (A) Bottom water $\Delta[CO_3^{2-}]$ vs. B/Ca ratios in three species of benthic foraminifera: *C. wuellerstorfi* (Yu and Elderfield, 2007), *N. umbonifera*, and *O. umbonatus*. *C. wuellerstorfi* and *O. umbonatus* data generated in this study are illustrated in light gray with error bars, while those generated by Rae et al. (2011) are depicted in dark gray. Data are fitted using both a standard least squares linear regression as well as a bivariate weighted least squares regression, which accounts for error in both the x- and y-axes (Reed, 1989; York, 1969). We estimated the error in seawater $\Delta[CO_3^{2-}]$ by averaging values from all stations within 2° of latitude and longitude of each core-top site and bootstrapped with replacement to obtain a standard deviation. Error bars reflect one standard deviation. The quantity sqrt(S/(n−2)) is a "goodness of fit" parameter and its expected value is unity. (B) Foraminiferal $\Delta[CO_3^{2-}]$ calculated from B/Ca using the bivariate weighted least squares regression equation shown in (A) vs. bottom water $\Delta[CO_3^{2-}]$ estimated from the GLODAP dataset. Solid lines in (A) represent linear fits for different species. In (B), both the 1:1 line (solid) and a ± 10 μmol/kg uncertainty envelope (dashed lines) are shown.

such that the overall sensitivity to seawater $\Delta[CO_3^{2-}]$ is similar (Fig. 3). The sensitivity to seawater $\Delta[CO_3^{2-}]$ is greater in the epifaunal *N. umbonifera* than in the shallow infaunal *O. umbonatus*, consistent with the low sensitivities observed in infaunal *Uvigerina* spp. and *Hoeglundina elegans* (Yu and Elderfield, 2007).

3.3. Eocene B/Ca

Co-occurring *N. truempyi* and *N. umbonifera* in 7 middle Eocene samples from ODP Sites 689, and 690 and 1262 show no consistent B/Ca differences between the two species (Fig. 6). Both species yielded B/Ca values ranging between 100 and 150 μmol/mol with a sum of the differences between species of −0.04 and with equal numbers above and below zero. Analyses of lower Eocene *N. truempyi* from Pacific (Site 1209) and Atlantic (Site 1263) cores show a similar range of B/Ca, though with a few values exceeding 200 μmol/mol. In contrast, the B/Ca of co-occurring *O. umbonatus* in both the middle and lower Eocene samples are consistently offset toward lower ratios by ~50–80 μmol/mol (Supplementary Fig. S1).

4. Discussion

4.1. Nuttallides umbonifera

B/Ca in *N. umbonifera* appears to be positively correlated with pH, $\Delta[CO_3^{2-}]$, BWT and $[B(OH)_4^-]/[HCO_3^-]$ and negatively with water depth (Fig. 4), but in most cases the correlation is not significant within all regions. For example, B/Ca in *N. umbonifera* does not co-vary consistently with deep water pH: in the Pacific and Southern Oceans, where B/Ca decreases with increasing water depth, core-top B/Ca varies by more than 30 μmol/mol while pH varies little (~7.76–7.77). This indicates that deep water pH does not completely explain *N. umbonifera* B/Ca,

and another parameter may be responsible for the 30 μmol/mol variability in the Pacific. Alternatively, there may not be sufficient variability in pH within the Pacific to show a significant relationship. Similar inferences can be made for the influence of temperature and $[B(OH)_4^-]/[HCO_3^-]$ on B/Ca, as bottom water temperatures in the Pacific cluster at ~1.5 °C whereas B/Ca ratios span more than 40 μmol/mol, and invariance in Pacific $[B(OH)_4^-]/[HCO_3^-]$ ratios (0.0185–0.0187 mol/mol) corresponds to a large spread in B/Ca. None of these parameters thus shows a consistently significant correlation with B/Ca, in agreement with Yu and Elderfield (2007).

In contrast, the correlation between benthic B/Ca and $\Delta[CO_3^{2-}]$ is consistent across multiple ocean basins, water temperatures and water depths with a sensitivity of B/Ca to $\Delta[CO_3^{2-}]$ of 1.23 ± 0.15 (Table 1, Figs. 3 and 4), comparable to that in *C. wuellerstorfi* (1.14; Yu and Elderfield, 2007). Based on 2 standard error on the regression, the uncertainty associated with reconstructing bottom water $\Delta[CO_3^{2-}]$ from *N. umbonifera* B/Ca is ~10 μmol/kg. Scatter may be due to bioturbation (i.e., mixing of tests of different ages) as well as to variability in foraminiferal B/Ca. For instance, the standard deviation of duplicate measurements of different sub-samples of foraminifera from a single sample averages ~5 μmol/mol (Yu and Elderfield, 2007) to as much as ~8 μmol/mol (this study). B/Ca in *N. umbonifera* is significantly correlated with deep water $\Delta[CO_3^{2-}]$ across a wide geographic range, thereby providing a robust basis for the reconstruction of past deep water saturation states. The calibration of this species extends the utility of this proxy into more corrosive waters and potentially into the Late Cretaceous (the stratigraphic range of *N. truempyi*).

4.2. Oridorsalis umbonatus

Our *O. umbonatus* sample size is small (n = 9), but the species' B/Ca values (~35–85 μmol/mol) are consistently lower than those in
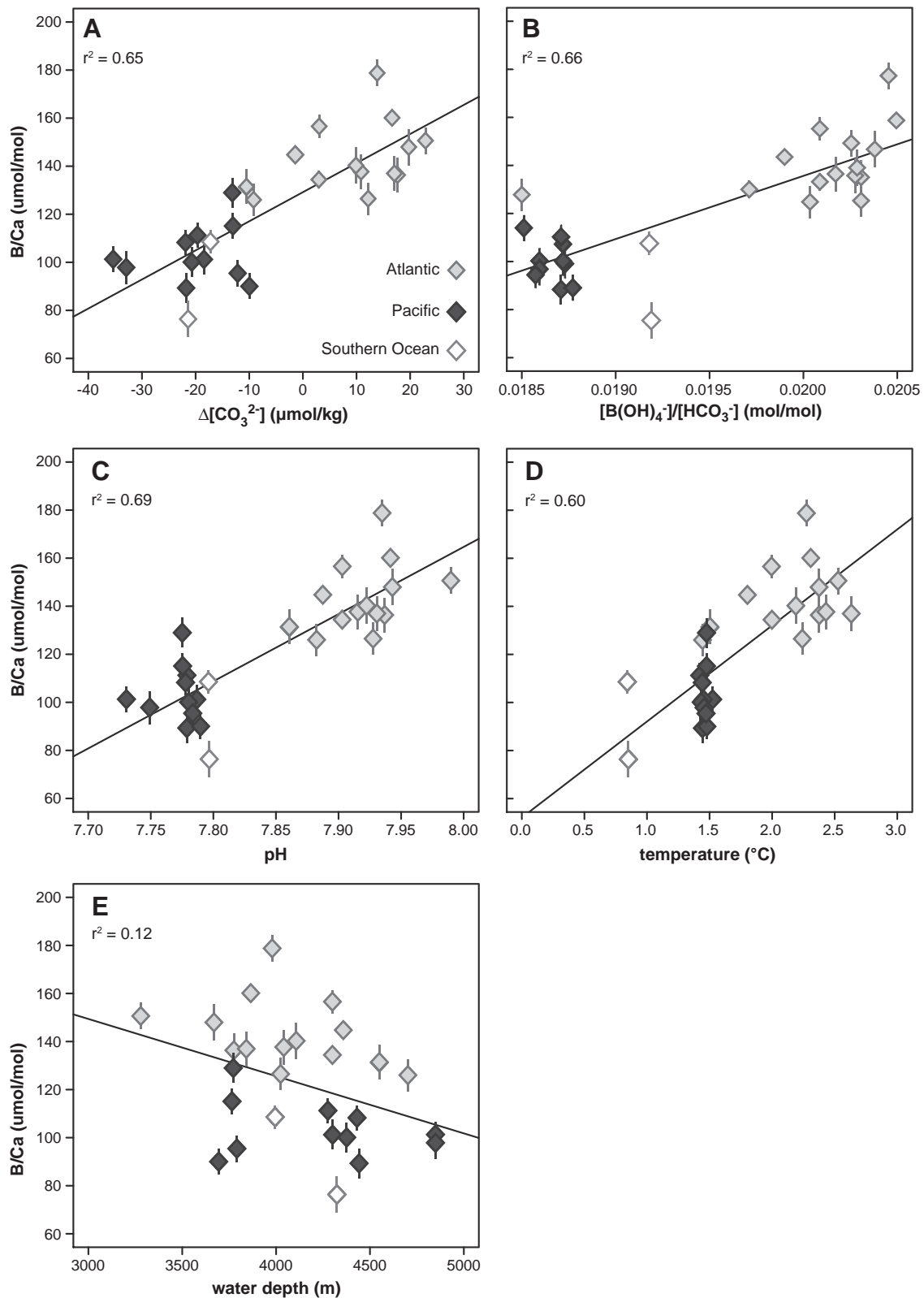
Fig. 4. *N. umbonifera* B/Ca ratios plotted vs. (A) $\Delta[CO_3^{2-}]$, (B) $[B(OH)_4^-]/[HCO_3^-]$, (C) pH, (D) BWT, and (E) water depth ($n = 27$). Seawater total B concentration, $[B]_{total}$, is calculated from salinity (S) by $[B]_{total}$ ($\mu mol/kg$) $= 416\ S/35$ (Uppstrom, 1974). While *N. umbonifera* B/Ca ratios appear to be correlated with all of the parameters investigated, only the correlation between benthic B/Ca and $\Delta[CO_3^{2-}]$ remains consistently robust across multiple ocean basins. Error bars reflect one standard deviation.

epifaunal species, even across a relatively wide range of seawater $\Delta[CO_3^{2-}]$ values (~ -20–40 $\mu mol/kg$), consistent with Rae et al. (2011). B/Ca in *O. umbonatus* appears to be largely insensitive to seawater $\Delta[CO_3^{2-}]$ ($R^2 = 0.31$, $p = 0.12$) and BWT ($R^2 = 0.14$, $p = 0.33$) (Fig. 5).

Correlations between B/Ca and pH ($R^2 = 0.53$, $p = 0.027$) or $[B(OH)_4^-]/[HCO_3^-]$ ($R^2 = 0.55$, $p = 0.023$) depend largely on one data point with a value of 85 $\mu mol/mol$, with all others between $\sim$35–55 $\mu mol/mol$. The B/Ca in this largely shallow infaunal (Rathburn
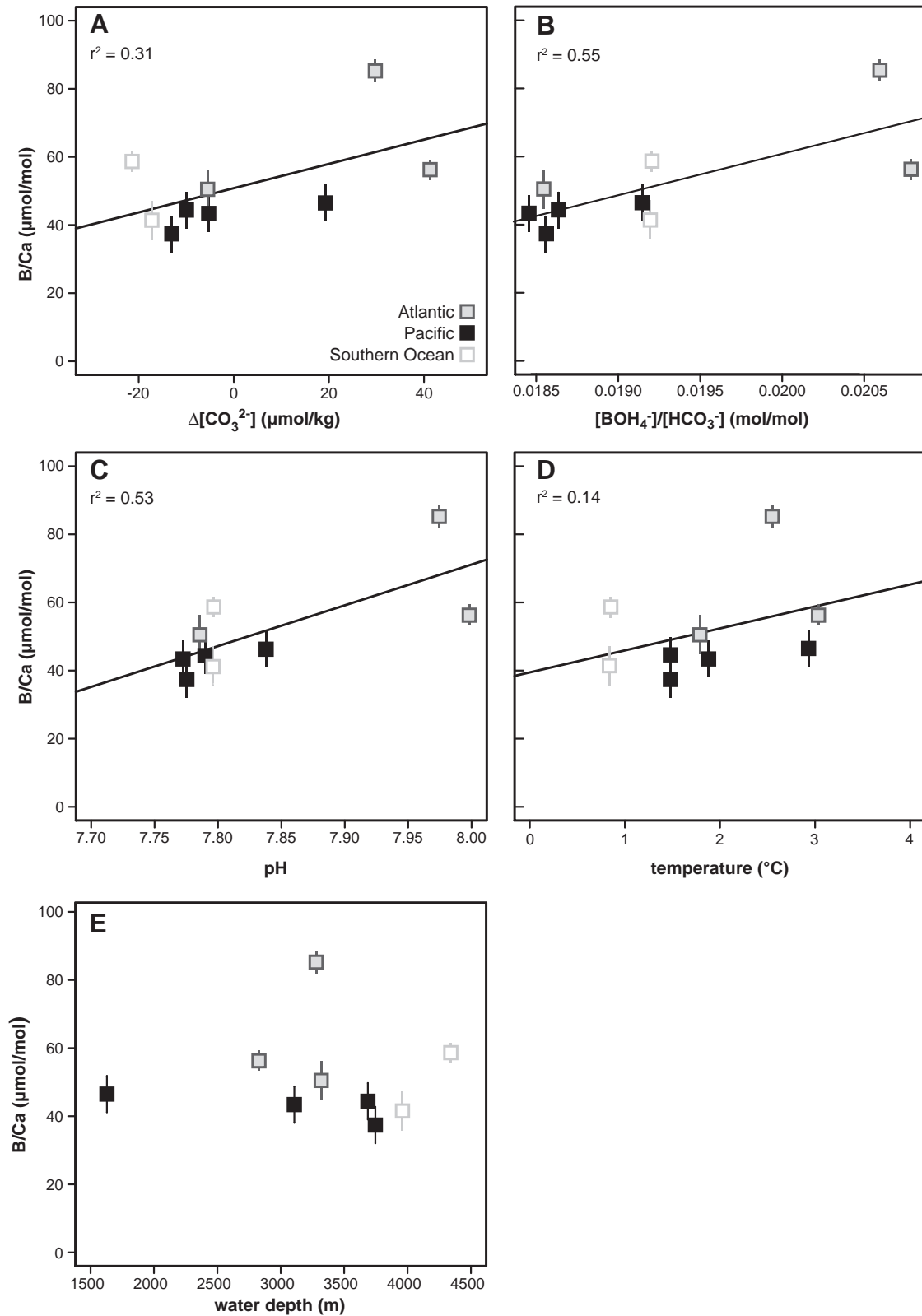
Fig. 5. *O. umbonatus* B/Ca ratios plotted vs. (A) $\Delta[CO_3^{2-}]$, (B) $[B(OH)_4^-]/[HCO_3^-]$, (C) pH, (D) BWT, and (E) water depth ($n=9$). Using a standard least squares fit, *O. umbonatus* B/Ca is moderately correlated with $[B(OH)_4^-]/[HCO_3^-]$ and pH, however the trend is highly dependent on just one data point (85 μmol/mol), with the remaining points clustering within a small range of B/Ca ratios (~35–55 μmol/mol). B/Ca ratios are also weakly correlated with $\Delta[CO_3^{2-}]$, however the sensitivity is too low (0.29 ± 0.2) for the use of this species to be recommended in paleo reconstructions.

and Corliss, 1994; Thomas and Shackleton, 1996) species probably reflects that this species calcified in contact with pore water rather than seawater, and thus cannot be used to reconstruct past bottom water $\Delta[CO_3^{2-}]$. A combination of B/Ca data from both *O. umbonatus* and *N. umbonifera* or another calibrated species could still be a useful indicator of saturation state, as the difference in B/Ca between such
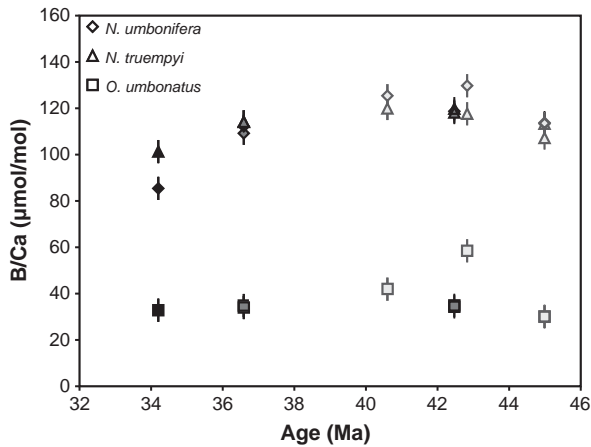
Fig. 6. B/Ca values in co-occurring *N. umbonifera*, *N. truempyi*, and *O. umbonatus* from middle Eocene samples from ODP Sites 689 (light gray), 690 (dark gray) and 1262 (black) plotted versus age (Ma) (Berggren et al., 1995).

species should be amplified or reduced at high vs. low saturation states. In addition, the difference between the two species provides a qualitative assessment of diagenetic overprinting, or the lack thereof, in older material.

4.3. Deep time: Calibration of Nuttallides truempyi

Extending the *N. umbonifera* B/Ca calibration into deep time using *N. truempyi*, an extinct species, involves a few assumptions that require testing. First and foremost, do both species incorporate B in a similar manner? Modern calibrations show that the relationship between B/Ca and $\Delta[CO_3^{2-}]$ is not the same for species within a genus. For example, *C. wuellerstorfi* and *C. mundulus* have noticeably different calibration slopes and intercepts (1.14x + 177 and 0.69x + 119, respectively; Yu and Elderfield, 2007). Such differences, in large part, may be explained by habitat preference; specifically, whether a species prefers the sediment/water interface or a few centimeters below will influence the $\Delta[CO_3^{2-}]$ to which it is regularly exposed, and in theory the B/Ca. For our calibration, $\Delta[CO_3^{2-}]$ is calculated for the overlying water and compared to both epifaunal and infaunal species. However, pore water saturation state deviates from bottom water $\Delta[CO_3^{2-}]$, particularly in sediments below $\Delta[CO_3^{2-}]$ depth (Bijma, et al., 2002; Sarmiento and Gruber, 2006), so that only the epifaunal species should exhibit a high sensitivity. This explains B/Ca patterns observed in *C. wuellerstorfi* and *C. mundulus*, with the former residing at the interface or on objects sticking out into the water column and the latter just a few cm below (0–4 cm) (e.g. Rathburn and Corliss, 1994). As such, *C. mundulus* as well as other infaunal taxa, for example *O. umbonatus* and *Uvigerina* spp, reside in waters that are more buffered with respect to saturation than the overlying waters.

Epifaunal *N. umbonifera* occupies a similar habitat as *C. wuellerstorfi* (e.g., Rathburn and Corliss, 1994) and thus shows a similar B/Ca vs $\Delta[CO_3^{2-}]$ sensitivity (this study). The presumption is that the extinct

N. truempyi occupied the same niche as well (Thomas, 1998). Our analyses of co-occurring *N. truempyi* and *N. umbonifera* from middle Eocene samples from Sites 689, 690 (Maud Rise) and 1262 (Walvis Ridge) show no consistent offset (Fig. 6), confirming this presumption. Moreover, co-existing *O. umbonatus* show roughly the same B/Ca offsets to both species of *Nuttallides* in Paleocene, Eocene, Glacial–Interglacial, and Holocene sediments (Fig. 6, Supplementary Fig. S1). The offset holds for B/Ca from high and low latitudes in the Pacific and Atlantic Oceans, lending credence to our assumption that the extinct *N. truempyi* occupied the same niche as *N. umbonifera* and their relationships to *O. umbonatus* have held throughout the Cenozoic.

The relative constancy in *Oridorsalis–Nuttallides* B/Ca over the last 55 Mya is noteworthy. It is beyond the scope of this paper to discuss this in detail, but one implication is for long-term stability of seawater B/Ca. Modeling suggests minimal change in the B concentration over the Cenozoic (~10%; Lemarchand et al., 2002), whereas Ca is thought to have declined overall (e.g. Horita et al., 2002), though by how much, and with how much superimposed variability, is debated (e.g. Fantle and dePaolo, 2005; Griffith et al., 2008). If so, all else being equal, we would expect oceanic B/Ca values to be higher at present than during the Eocene. Because the ratio is about the same or slightly lower, this might imply a compensating effect in carbonate saturation, though further research is required for a full investigation of this idea.

5. Status of the benthic B/Ca proxy

The relationship between B/Ca and $\Delta[CO_3^{2-}]$ in benthic foraminifera is empirical, but significant, and thus can serve as a proxy for past deep water saturation state. Use of this proxy should include constraints on water depth, BWT and salinity (the latter not usually important in the deep sea but potentially in shallower waters), and involve other carbonate system proxies such as carbonate content, fragmentation, and shell mass indexes. The application of the B/Ca proxy in deep time also requires consideration of past variations in both the boron and calcium concentrations in seawater ($[B]_{sw}$ and $[Ca]_{sw}$, respectively). Because the residence time of boron in seawater is long (15–20 My, Lemarchand et al., 2000, 2002), changes in $[B]_{sw}$ can be assumed constant over intervals that are short relative to its residence time. In addition, the theory behind the proxy assumes that borate, not boric acid, is incorporated into the tests of foraminifera. Nuclear magnetic resonance (NMR) data, however, indicate that both trigonal boric acid and tetrahedral borate are present at almost equal abundance in biogenic calcite and aragonite (Klochko et al., 2009), and we do not know whether seawater boric acid is entering the crystal lattice, or borate is converted to boric acid internally. Nonetheless, the variance in benthic foraminiferal B/Ca with seawater carbonate chemistry appears to be robust, and should prove useful for constraining past variations at longer time scales than glacial–interglacial time-scales (Yu et al., 2010a, b).

6. Down-core application of the N. umbonifera calibration

Past deep-water $\Delta[CO_3^{2-}]$ can be calculated using down-core values (Yu et al., 2008):

$$\Delta\left[CO_3^{2-}\right] = \Delta\left[CO_3^{2-}\right]_{pre-industrial} + \Delta(B/Ca)/\text{sensitivity} \qquad (1)$$

where $\Delta[CO_3^{2-}]_{pre-industrial}$ is the pre-industrial $\Delta[CO_3^{2-}]$ value (Key et al., 2004), $\Delta(B/Ca)$ is the change in B/Ca in down-core samples relative to the core-top B/Ca value (preferably an average of the top three samples), and sensitivity is the calibrated sensitivity of B/Ca to $\Delta[CO_3^{2-}]$ (1.35 µmol/mol per µmol/kg for *N. umbonifera*). In

Table 1
Regression between bottom water $\Delta[CO_3^{2-}]$ and B/Ca ratios measured in *N. umbonifera* and *O. umbonatus* from Holocene core tops. Species are fitted to the form B/Ca = a $\Delta[CO_3^{2-}]$ + b using a bivariate least squares regression that accounts for uncertainty in both the x- and y-axes (Reed, 1989; York, 1969). The quantity sqrt(S/(n−2)) is a "goodness of fit" parameter and its expected value is unity.

Species	a	b	n	sqrt(S/n-2)
N. umbonifera	1.23 ± 0.15	134 ± 2.7	27	2.9
O. umbonatus	0.29 ± 0.2	56.4 ± 5.5	9	4.1

this way, Yu et al. (2008) avoided complications due to the uncertainties in hydrographic data. Paleo-$[CO_3^{2-}]$ can then be calculated by:

$$\left[CO_3^{2-}\right] = \Delta\left[CO_3^{2-}\right] + \left[CO_3^{2-}\right]_{sat} \qquad (2)$$

when $[CO_3^{2-}]_{sat}$ can be constrained. $[CO_3^{2-}]_{sat}$ is influenced by salinity (S), pressure (P), and BWT, which collectively have a close to negligible effect on $[CO_3^{2-}]_{sat}$ on glacial/interglacial timescales (Yu et al., 2008), so that pre-industrial values can be used to calculate $[CO_3^{2-}]$. In deeper time, it is important to constrain these variables using other proxies (e.g. $\delta^{18}O$, Mg/Ca) along with numerical models (e.g., Zeebe and Zachos, 2007) to estimate $[CO_3^{2-}]_{sat}$. Relative changes in B/Ca ratios can provide semi-quantitative constraints on changes in bottom water $[CO_3^{2-}]$, but quantitative estimates of past deep-water $[CO_3^{2-}]$ will likely require a multi-proxy approach.

7. Conclusion

B/Ca in *N. umbonifera* is significantly, positively correlated with deep-water saturation state, and the relationship between B/Ca and $\Delta[CO_3^{2-}]$ remains consistent across all investigated ocean basins, water depths and temperatures. $\Delta[CO_3^{2-}]$ is the only variable considered for which this is true, suggesting that B/Ca ratios in *N. umbonifera*, like those in *C. wuellerstorfi*, can serve as a proxy for past deep-water saturation states. Application of the proxy requires use of an optimum calibration line, which we calculated by means of a bivariate least squares regression incorporating errors along both axes. We demonstrate that co-occurring middle Eocene *N. umbonifera* and *N. truempyi* do not have significantly different B/Ca, and therefore this core-top calibration extends the utility of the B/Ca proxy beyond glacial–interglacial timescales into deeper time, as well as into more corrosive waters not inhabited by other calibrated species. Because of its infaunal habitat, B/Ca in *O. umbonatus* is largely insensitive to bottom water $\Delta[CO_3^{2-}]$, and cannot be used for reconstruction of saturation states (e.g. Yu and Elderfield, 2007). It does, however, hold promise for constraining long-term changes in seawater B/Ca.

Supplementary materials related to this article can be found online at doi:10.1016/j.epsl.2011.08.023.

References

Al-Ammar, A., Gupta, R.K., Barnes, R.M., 1999. Elimination of boron memory effect in inductively coupled plasma-mass spectrometry by addition of ammonia. Spectrochim. Acta, Part B 54, 1077–1084.
Al-Ammar, A., Reitznerova, E., Barnes, R.M., 2000. Improving boron isotope ratio measurement precision with quadrupole inductively coupled plasma-mass spectrometry. Spectrochim. Acta, Part B 55, 1861–1867.
Bassinot, F.C., Melieres, F., Gehlen, M., Levi, C., Labeyrie, L., 2004. Crystallinity of foraminifera shells: a proxy to reconstruct past bottom water CO$\overline{_3}$ changes? Geochem. Geophys. Geosyst. 5, Q08D10.
Berggren, W.A., Kent, D.V., Swisher III, C.C., Aubry, M., 1995. A revised Cenozoic geochronology and chronostratigraphy. Geochronology, Time Scales and Global Stratigraphic Correlation: In: Berggren, W.A., et al. (Ed.), SEPM Special Publication, 54, pp. 129–212.

Bijma, J., Hönisch, B., Zeebe, R., 2002. Impact of ocean carbonate chemistry on living foraminiferal shell weight: comment on "Carbonate ion concentration in glacial-age deep waters of the Carribbean Sea" by W.S Broecker and E. Clark. Geochem. Geophys. Geosyst. 3 (11).
Boyle, E., Keigwin, L.D., 1985. Comparison of Atlantic and Pacific paleochemical records for the last 215,000 years — changes in deep ocean circulation and chemical inventories. Earth Planet. Sci. Lett. 76 (1–2), 135–150.
Bremer, M.L., Lohmann, G.P., 1982. Evidence for primary control of the distribution of certain Atlantic Ocean benthonic foraminifera by degree of carbonate saturation. Deep-Sea Res. 2, 987–998.
Broecker, W., Clark, E., 1999. CaCO$_3$ size distribution: a paleocarbonate ion proxy? Paleoceanography 14 (5), 596–604.
Broecker, W., Clark, E., 2003. Glacial-age deep sea carbonate ion concentrations. Geochem. Geophys. Geosyst. 4, 1047.
Cantrell, C.A., 2008. Technical note: review of methods for linear least-squares fitting of data and application to atmospheric chemistry problems. Atmos. Chem. Phys. 8, 5477–5487.
de Villiers, S., Greaves, M., Elderfield, H., 2002. An intensity ratio calibration method for the accurate determination of Mg/Ca and Sr/Ca of marine carbonates by ICP-AES. Geochem. Geophys. Geosyst. 3 (1), 1001.
Dickens, G., Castillo, M., Walker, J., 1997. A blast of gas in the latest Paleocene: simulating first-order effects of massive dissociation of oceanic methane hydrate. Geology 25 (3), 259–262.
Efron, B., 1979. Bootstrap methods: another look at the jackknife. Ann. Stat. 7 (1), 1–26.
Fabry, V.J., Seibel, B.A., Feely, R.A., Orr, J.C., 2008. Impacts of ocean acidification on marine fauna and ecosystem processes. ICES J. Mar. Sci. 65 (3), 414–432.
Fantle, M.S., dePaolo, D.J., 2005. Variations in the marine Ca cycle over the past 20 million years. Earth Planet. Sci. Lett. 237 (1–2), 102–117.
Feely, R.A., 2004. Impact of anthropogenic CO$_2$ on the CaCO$_3$ system in the oceans. Science 305 (5682), 362–366.
Foster, G.L., 2008. Seawater pH, pCO$_2$ and $[CO_3^{2-}]$ variations in the Caribbean Sea over the last 130 kyr: a boron isotope and B/Ca study of planktic foraminifera. Earth Planet. Sci. Lett. 271 (1–4), 254–266.
Griffith, E.M., Paytan, A., Caldeira, K., Bullen, T.D., Thomas, E., 2008. A dynamic marine calcium cycle during the past 28 million years. Science 322, 1671–1674. doi:10.1126/science.1163614.
Hemming, N.G., Hanson, G.N., 1992. Boron isotopic composition and concentration in modern marine carbonates. Geochim. Cosmochim. Acta 56 (1), 537–543.
Horita, J., Zimmermann, H., Holland, H.D., 2002. Chemical evolution of seawater during the Phanerozoic: implications from the record of marine evaporites. Geochim. Cosmochim. Acta 66 (21), 3733–3756.
Kaiho, K., 1998. Phylogeny of deep-sea calcareous trochospiral benthic Foraminifera: evolution and diversification. Micropaleontology 44, 291–311.
Key, R., Kozyr, A., Sabine, C., Lee, K., 2004. A global ocean carbon climatology: results from Global Data Analysis Project (GLODAP). Global Biogeochem. Cycles 18, GB4031.
Key, R.M., Tanhua, T., Olsen, A., Hoppema, M., Jutterström, S., Schirnick, C., van Heuven, S., Kozyr, A., Lin, X., Velo, A., Wallace, D., Mintrop, L., 2010. The CARINA data synthesis project: introduction and overview. Earth Syst. Sci. Data 2, 105–121.
Klochko, K., Cody, G., Tossell, J., Dera, P., 2009. Re-evaluating boron speciation in biogenic calcite and aragonite using ^{11}B MAS NMR. Geochim. Cosmochim. Acta 73, 1890–1900.
Kromer, P., Least Squares Fitting in Excel with Error in Both VariablesLast accessed February 6, 2011, from http://vizsage.com/other/leastsquaresexcel/.
Lemarchand, D., Gaillardet, J., Lewin, E., Allegre, C.J., 2000. The influence of rivers on marine boron isotopes and implications for reconstructing past ocean pH. Nature 408, 951–954.
Lemarchand, D., Gaillardet, J., Lewin, E., Allegre, C.J., 2002. Boron isotope systematics in large rivers: implications for the marine boron budget and paleo-pH reconstruction over the Cenozoic. Chem. Geol. 190, 123–140.
Lohmann, G.P., 1995. A model for variation in chemistry of planktonic foraminifera due to secondary calcification and selective dissolution. Paleoceanography 10 (3), 445–457.
Marchitto, T.M., Curry, W.B., Oppo, D.W., 2000. Zinc concentrations in benthic foraminifera reflect seawater chemistry. Paleoceanography 15 (3), 299–306.
Marchitto, T.M., Oppo, D.W., Curry, W.B., 2002. Paired benthic foraminiferal Cd/Ca and Zn/Ca evidence for a greatly increased presence of Southern Ocean Water in the glacial North Atlantic. Paleoceanography 17 (3), 1038.
Martin, P.A., Lea, D.W., 2002. A simple evaluation of cleaning procedures on fossil benthic foraminiferal Mg/Ca. Geochem. Geophys. Geosyst. 3, 8401.
Pelletier, G., Lewis, E., Wallace, D., 2007. CO2sys.xls: a calculator for the CO$_2$ system in seawater for Microsoft Excel/VBA. Washington State Department of Ecology, Olympia, WA, USA.
Rae, J.W.B., Foster, G.L., Schmidt, D.N., Elliott, T., 2011. Boron isotopes and B/Ca in benthic foraminifera: proxies for the deep ocean carbonate system. Earth Planet. Sci. Lett. 302 (3–4), 403–413.
Rathburn, A.E., Corliss, J.B., 1994. The ecology of living (stained) deep-sea benthic foraminifera from the Sulu Sea. Paleoceanography 9, 87–150.
Reed, B.C., 1989. Linear least-squares fits with errors. Am. J. Phys. 57 (7), 642–646.
Riebesell, U., Zondervan, I., Rost, B., Tortell, P.D., Zeebe, R., Morel, F.M.M., 2000. Reduced calcification of marine plankton in response to increased atmospheric CO2. Nature 407, 364–367.
Rosenthal, Y., Field, M.P., Sherrell, R.M., 1999. Precise determination of element/calcium ratios in calcareous samples using sector field inductively coupled plasma mass spectrometry. Anal. Chem. 71, 3248–3253.
Sarmiento, J.L., Gruber, N., 2006. Calcium carbonate cycle. Ocean Biogeochemical Dynamics. Princeton University Press, Princeton, NJ. 503 pp.
Schweizer, M., 2006. Evolution and molecular phylogeny of Cibicides and Uvigerina (Rotaliida, Foraminifera). Geological Ultraiectina261, 168 http://igitur-archive.library.uu.nl/dissertations/2006-0606-200952/index.htm.

Shackleton, N.J., 2000. The 100,000-year ice-age cycle identified and found to lag temperature, carbon dioxide, and orbital eccentricity. Science 289, 1897–1902.

Thomas, E., 1998. The biogeography of the late Paleocene benthic foraminiferal extinction. In: Aubry, M.-P., Lucas, S., Berggren, W.A. (Eds.), Late Paleocene–early Eocene Biotic and Climatic Events in the Marine and Terrestrial Records. Columbia University Press, pp. 214–243.

Thomas, E., Shackleton, N.J., 1996. The Palaeocene–Eocene benthic foraminiferal extinction and stable isotope anomalies. Geol. Soc. London Spec. Publ. 101, 401–441.

Uppstrom, L.R., 1974. The boron/chlorinity ratio of deep-sea water from the Pacific Ocean. Deep-Sea Res. 21, 161–162.

van Morkhoven, F.P.C.M., Berggren, W.A., Edwards, A.S. (Eds.), 1986. Cenozoic Cosmopolitan Deep-Water Benthic Foraminifera. Bulletin des Centres de Recherches Exploration-Production Elf-Aquitaine 11. Pau. 421 pp.

Wara, M., Delaney, M., Bullen, T., Ravelo, A.C., 2003. Possible roles of pH, temperature, and partial dissolution in determining boron concentration and isotopic composition in planktonic foraminifera. Paleoceanography 18 (4), 1100.

York, D., 1969. Least squares fitting of a straight line with correlated errors. Earth Planet. Sci. Lett. 5, 320–324.

York, D., Evensen, N.M., López Martínez, M., De Basabe Delgado, J., 2004. Unified equations for the slope, intercept, and standard errors of the best straight line. Am. J. Phys. 72 (3), 367–375.

Yu, J., Day, J., Greaves, M., Elderfield, H., 2005. Determination of multiple element/ calcium ratios in foraminiferal calcite by quadrupole ICP-MS. Geochem. Geophys. Geosyst. 6, Q08P01.

Yu, J., Elderfield, H., Hönisch, B., 2007. B/Ca in planktonic foraminifera as a proxy for surface seawater pH. Paleoceanography 22 (2), PA2202.

Yu, J., Elderfield, H., 2007. Benthic foraminiferal B/Ca ratios reflect deep water carbonate saturation state. Earth Planet. Sci. Lett. 258 (1–2), 73–86.

Yu, J., Elderfield, H., Piotrowski, A., 2008. Seawater carbonate ion-δ^{13}C systematics and application to glacial–interglacial North Atlantic ocean circulation. Earth Planet. Sci. Lett. 271, 209–220.

Yu, J., Broecker, W.S., Elderfield, H., Jin, Z., McManus, J., Zhang, F., 2010a. Loss of carbon from the deep sea since the last glacial maximum. Science 330 (6007), 1084–1087.

Yu, J., Foster, G., Elderfield, H., Broecker, W.S., Clark, E., 2010b. An evaluation of benthic foraminiferal B/Ca and δ11B for deep ocean carbonate ion and pH reconstructions. Earth Planet. Sci. Lett. 293 (1–2), 114–120.

Zeebe, R., Zachos, J.C., Dickens, G.R., 2009. Carbon dioxide forcing alone insufficient to explain Palaeocene–Eocene thermal maximum warming. Nat. Geosci. doi:10.1038/ NGEO578.

Zeebe, R., Zachos, J.C., 2007. Reversed deep-sea carbonate ion basin gradient during Paleocene–Eocene thermal maximum. Paleoceanography 22 (PA3201), 1–17.

Zeebe, R.E., Wolf-Gladrow, 2001. CO$_2$ in Seawater: Equilibrium, Kinetics, Isotopes: Elsevier Oceanography Series, Amsterdam, 65. 346 pp.